ELSEVIER

Thin Solid Films 398–399 (2001) 361–367

thin solid films

www.elsevier.com/locate/tsf

Junction properties of nickel phthalocyanine thin film devices utilising indium injecting electrodes

T.S. Shafai*, T.D. Anthopoulos

Staffordshire University, School of Engineering and Advanced Technology, Beaconside, Stafford, ST18 ODF, UK

Abstract

The d.c. electrical properties of gold/nickel phthalocyanine/indium (Au/NiPc/In) thin film structures have been investigated. Three-layered devices were fabricated utilising a sequential vacuum sublimation technique. At low voltages, current density in the forward direction was found to obey the diode equation, while for higher voltage levels, conduction was dominated by a space-charge-limited conduction (SCLC) mechanism. In the reverse bias direction a transition from electrode-limited to a bulk-limited conduction process was identified. After prolonged exposure of the sample to dry air a weak polarity dependence of conduction was observed. Analysis of the experimental data under reverse bias suggests a transition from electrode-limited to a bulk-limited conduction process for lower and higher applied voltages, respectively. After annealing of the samples at 393 K in vacuum for 20 min, a strong rectifying behaviour was evident. Results were interpreted in terms of an O_2 adsorption process at the NiPc/In interface. Hole trapping parameters together with various junction properties have been also reported and analysed.

Keywords: d.c. electrical properties; Au/NiPc/In thin film structures; Three-layered devices

1. Introduction

In recent years organic semiconducting materials are rapidly making an impact in the area of electronics and optoelectronics. During the last 10 years, phthalocyanine (H_2Pc) and its metal derivatives (MPcs) have received increasing attention due to their potentials for applications in the areas of gas sensing [1], photovoltaics (PV) [2], and organic electroluminescent devices (OLEDs) [3]. One of the major advantages of using phthalocyanines is their chemical stability as well as the ability to readily modify the molecular structure allowing the molecular engineering of their physical properties accordingly. In general, Pc and MPcs are classified as p-type semiconductors characterised by low mobility and low carrier concentration [4]. It is well established that when suitable electrode materials are employed formation of a Schottky-type contact between metal electrode and Pc-MPcs is possible [5,6]. In addition, the electrical properties of phthalocyanine-based devices are also known to be critically dependent not only on the electrode material employed but also upon the ambient conditions. For example, exposure to oxidising gases such as O_2 increases the conductivity by several orders of magnitude; hence in the presence of a Schottky barrier enhancement of the contact potential may be achieved. Loutfy et al. have reported that O_2 enhances the power conversion efficiency of organic photovoltaic cells [7]. Previous work on nickel phthalocyanine (NiPc) thin films has reported a relatively high mobility value ($\sim 1\times10^{-5}$ m^2 V^{-1} s^{-1}) [8], when compared with mobility values reported for several other Pc compounds (7.6×10^{-9} m^2 V^{-1} s^{-1} [9], 3×10^{-7} m^2 V^{-1} s^{-1} [10] and 10^{-8} m^2 V^{-1} s^{-1} [11]). This particular feature makes NiPc a potential candidate for development of futures electronic devices.

In the present paper, the dark electrical characteristics of freshly prepared Au/NiPc/In devices are studied. The effects of prolonged exposure of the sample to dry

* Corresponding author. Tel.: +44-1785-353240; fax: +44-1785-353552.

E-mail address: t.sadat-shafai@staffs.ac.uk (T.S. Shafai).

0040-6090/01/$ - see front matter
PII: S0040-6090(01)01345-1

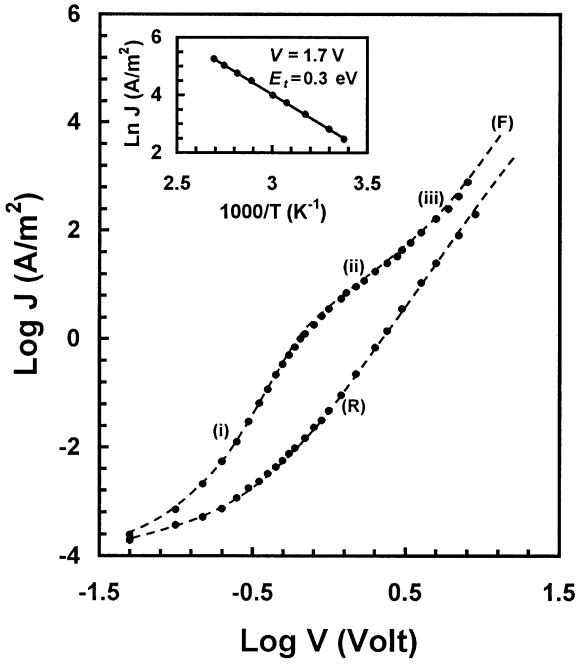

Fig. 1. Typical set of the *J–V* characteristics obtained from a freshly prepared Au/NiPc/In sample maintained at room temperature under high vacuum conditions. For forward (F) and reverse (R) bias.

air are reported and analysed. The influence of thermal annealing is also investigated.

2. Experimental details

Multilayer devices consisting of Au/NiPc/In were fabricated under high vacuum (10^{-4} Pa). Details on purification, deposition techniques and substrates employed are similar to those reported previously [12]. Gold (electrode thickness ~80 nm) was chosen because it is known to provide Ohmic contact with most Pcs [4]. Thickness of the organic layer was ~0.5 μm. Indium electrodes were sublimed utilising molybdenum boats at an evaporation rate of 0.4 nm s^{-1}, to an overall thickness of 80 nm. The effective conduction area of each device (A) was ~1.2×10^{-5} m^2. Fresh samples were then transferred to a subsidiary vacuum system, and maintained under high vacuum for several hours prior to electrical measurements. Electrical characterisation of the devices was performed in a dark enclosure using a conventional d.c. technique, utilising a Thurlby PL320 TGP stabilised power supply, a Keithley 414S picoammeter and an HP 3478A voltmeter. The polarity of the forward bias in all electrical measurements was made positive at the gold electrode. In order to study the effects of O_2 doping, devices were exposed to dry air for a period of 3 days. The effects of temperature on the conduction mechanisms were investigated using a micro heater located underneath the sample of interest.

3. Results and discussion

3.1. Freshly prepared samples

Fig. 1 shows a typical set of the dark *J–V* characteristics, under forward and reverse bias for an Au/NiPc/In device maintained at room temperature in vacuum. Under forward bias and within the narrow voltage range of 0.075–0.25 V, current density (J) obeys the thermionic emission equation given by Sze [13] as

$$J = J_s\left(\exp\left(\frac{eV}{nkT}\right) - 1\right) \quad (1)$$

where e is the electronic charge, V is the applied voltage across the device, k is the Boltzmann's constant, T is the absolute temperature, and n the diode ideality factor. In Eq. (1) J_s is the saturation current density and can be expressed as

$$J_s = A^{**}T^2\exp\left(-\frac{e\phi_b}{kT}\right) \quad (2)$$

where A^{**} is the Richardson constant, and ϕ_b the barrier height at the NiPc/In interface. A semi-logarithmic plot of the forward current density vs. applied voltage for the same set of devices is shown in Fig. 2. For applied voltages within the range of 0.075–0.25 V, current density (J) increases exponentially. The extrapolated intercept of the linear portion of the graph with the J axis, at $V=0$ V, yields the value for $J_s \sim 9.6\times10^{-5}$ Am^{-2}. Using the graphically obtained value for J_s and a value of A^{**} ~1.3×10^5 Am^{-2} K^{-2}, as derived from

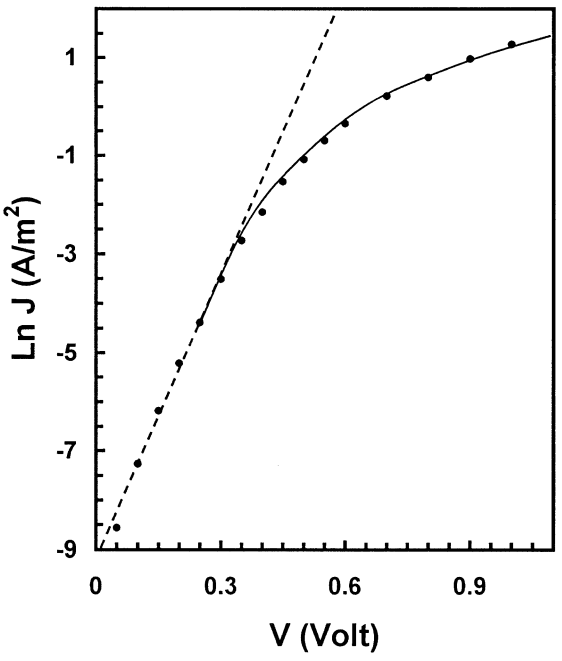

Fig. 2. Semi-logarithmic plot of the forward bias *J–V* characteristic obtained from the sample shown in Fig. 1.

our earlier work, together with Eq. (2) a value of $\phi_b = 0.82$ eV was derived. The ideality factor n was also calculated from Eq. (1), yielding a value of 1.9. Deviations of n from unity may be attributed to either recombination of electrons and holes in the depletion region, and/or the increase of the diffusion current due to increasing applied voltage. Rectification ratio (RR) of the devices calculated at ± 1 V yields a value of RR ≈ 80. At higher applied voltages (Fig. 1, curve f), current density shows two different power law exponents of the form

$$J \propto V^m \tag{3}$$

Within the voltage range of 1–2.5 V (region ii), a quadratic dependence of current density on voltage is observed, suggesting a SCLC conduction mechanism characterised by a single trapping level. The current density under these circumstances is given by Rose [14] as

$$J = \frac{9}{8}\varepsilon\mu\theta\frac{V^2}{d^3} \tag{4}$$

where ε and μ are the permittivity and carrier mobility of NiPc respectively, and d the thickness of NiPc layer. In Eq. (4) θ is the ratio of free to trapped charges and is given as

$$\theta = \frac{N_v}{N_{t(s)}}\exp\left(-\frac{E_t}{kT}\right) \tag{5}$$

In addition to the symbols defined previously N_v is the effective density of states, $N_{t(s)}$ is the total trap concentration, and E_t the energetic position of the single trap level above the valence band edge. From region (i) of the forward bias characteristic in Fig. 1, a value of $\theta = 2.86\times10^{-4}$ is obtained. Temperature measurements (shown in the left-hand corner of Fig. 1) in this region indicates a value for $E_t = 0.35$ eV. Previous work on copper phthalocyanine (CuPc) thin films has indicated a value for effective density of states $N_v = 10^{27}$ m^{-3} [15]. This value corresponds approximately to one electronic state per molecule. Since the molecular size and crystalline structure of NiPc and CuPc are very similar [16], the same value for the effective density of states in the valence band edge was adopted. Therefore, utilising these values for θ, E_t and N_v, Eq. (5) yields the value for $N_{t(s)} = 3.74\times10^{24}$ m^{-3}. The latter falls within the range of previously reported values from this laboratory for Au/NiPc/Au structures [12]. For higher applied voltages ($V > 6$ V) a $J \propto V^{3.75}$ relation is observed. Such power dependence indicates a SCLC characterised by an exponential distribution of trapping levels. The relationship of J as a function of V for this particular case is given by Lampert [17] as

$$J_{SCLC} = e\mu N_v\left(\frac{\varepsilon}{eP_0kT_t}\right)^l\frac{V^{l+1}}{d^{2l+1}} \tag{6}$$

where P_0 is the trap concentration per unit energy range at the valence band edge $(l+1)$ represents the power law exponent, where $l = T_t/T$, with T_t a temperature parameter characterising the exponential trap distribution given by the relation

$$P(E) = P_0\exp\left(\frac{-E}{kT_t}\right) \tag{7}$$

In Eq. (7), $P(E)$ is the trap concentration per unit energy range as a function of energy E above the valence band edge. The total trap concentration of trap distribution $N_{t(e)}$, has been given by Gould and Rahman [18] as

$$N_{t(e)} = P_0kT_t \tag{8}$$

From Eq. (6), a slope of 3.75 implies that $l = 2.75$, thus, yielding the temperature parameter $T_t = 860$ K, for $T_t = 293$ K. From previous work in this laboratory a value for the hole mobility μ equal to 7×10^{-5} m^{-1} V^{-1} s^{-1}, was evaluated. A fuller analysis of the particular technique employed for calculation of this parameter has been reported elsewhere [19]. Using the derived value for μ and considering the same value for N_v, Eqs. (6) and (8) yield the following values, $P_0 = 4.75\times10^{44}$ J^{-1} m^{-3} and $N_{t(e)} = 5.28\times10^{24}$ m^{-3}. Derived values are comparable in magnitude with values reported previously by Abdel-Malik [20], for thin films of NiPc utilising gold and aluminium electrodes. In comparison to the work of Gould and Blyth [21], values for P_0 and $N_{t(e)}$ were approximately two orders of magnitude higher. This discrepancy may be explained in terms of NiPc deposition conditions, as well as on the degree of purity of the materials employed. Under reverse bias conditions, the J–V characteristic in Fig. 1 exhibits lower current levels when compared with the J–V characteristic obtained under forward bias, indicating the existence of a current limitation mechanism, induced either by the Schottky or the Poole–Frenkel effect. Current density–voltage expressions for both mechanisms are given by Simmons [22] as

$$J = A^{**}T^2\exp\left(-\frac{\phi_s}{kT}\right)\exp\left(\frac{\beta_S V^{1/2}}{kTd^{1/2}}\right) \tag{9}$$

for the Schottky effect, and

$$J = J_0\exp\left(\frac{\beta_{PF}V^{1/2}}{kTd^{1/2}}\right) \tag{10}$$

for the Poole–Frenkel effect. In Eqs. (9) and (10), ϕ_S is the Schottky barrier height at the injecting electrode interface, J_0 $(=\sigma_0 F)$ is the low-field current density, and β_S and β_{PF} are, respectively, the Schottky and Poole–Frenkel field-lowering coefficients. Theoretical

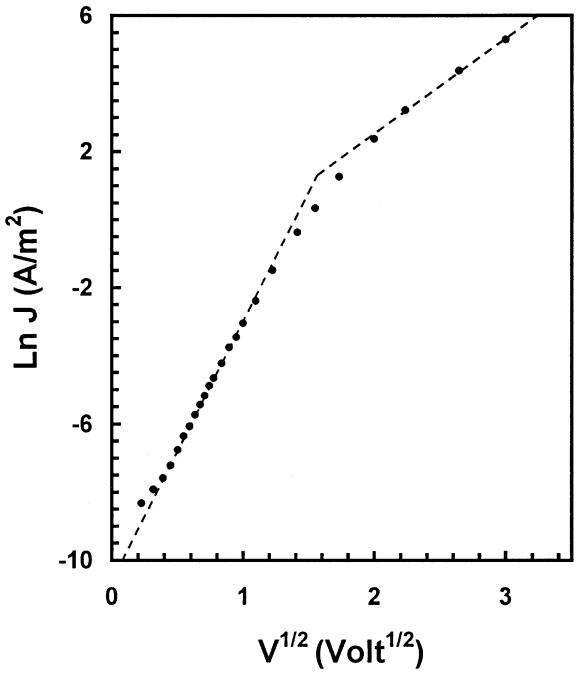

Fig. 3. Semi-logarithmic plot of the reverse *J–V* characteristic for a freshly prepared Au/NiPc/In sample maintained at room temperature under high vacuum conditions.

values for both β_S and β_{PF} are given by

$$2\beta_S = \beta_{PF} = \left(\frac{e^3}{\pi\varepsilon}\right)^{1/2} \quad (11)$$

Since $\varepsilon = 2.425\times10^{-11}$ F m^{-1} [12], the theoretical values of $\beta_S = 2.29\times10^{-5}$ eV m$^{1/2}$ V$^{-1/2}$ and $\beta_{PF} = 4.58\times10^{-5}$ eV m$^{1/2}$ V$^{-1/2}$ were calculated. It is evident from Eqs. (9) and (10) that the experimental values for the coefficient β can be obtained by plotting the reverse bias characteristic in the form of ln (J) vs. $V^{1/2}$. Fig. 3 shows the reverse bias data re-plotted in this form. It can be seen from the figure that the curve consists of two distinct linear sections. From the slope of the low voltage section a value of $\beta = 13.2\times10^{-5}$ eV m$^{1/2}$ V$^{-1/2}$ was derived. A value for the coefficient β was also calculated from the gradient of the linear portion of the curve in the higher voltage range, yielding a value of $\beta = 5.8-10^{-5}$ eV m$^{1/2}$ V$^{-1/2}$. Similar findings have been reported previously for Pc films utilising aluminium injecting electrodes [23], and were interpreted in terms of the Schottky and Poole–Frenkel effect, respectively. In the lower voltage region of Fig. 1, conductivity exhibits strong polarity dependence indicating a current limitation mechanism originated from the NiPc/In interface rather than the bulk of NiPc. Nevertheless, the derived value of β from the lower voltage region is at variance with that expected for the Schottky effect, being 5.76 times the theoretical value for β_S. This difference may be attributed to a thermally assisted tunnelling field emission of carriers occurring at the peak of the barrier where the effective barrier width is very narrow. Alternatively, other workers [5,6] have explained this difference in terms of a Schottky depletion region extending only in a distance d_S and not across the entire Pc layer, while assuming the theoretical value of β_S in Eq. (9). Using the above mentioned theoretical value of β_S in Eq. (9), together with the slope and the *y*-intercept of the lower voltage region in Fig. 3, values for $\phi_S = 0.84$ eV and $d_S = 15$ nm, were calculated. The former value is in good agreement with the value of ϕ_b derived previously from Fig. 2, thus, providing further experimental evidence of its magnitude. Derived value for d_S fall within the range of previously reported values [24,25]. The value of β derived from the higher voltage range is in good agreement with that expected for the Poole–Frenkel effect being 1.3 times the theoretical value of β_{PF}. This difference may be attributed to the non-uniform electric field within the bulk of the NiPc layer [26].

3.2. Oxygen-doped samples

Fig. 4 shows the typical *J–V* characteristics of an Au/NiPc/In sample after it has been exposed to dry air for 3 days under atmospheric pressure. It can be seen that a significant decrease in conductivity continues throughout the measurements, for both forward and reverse bias conditions. The latter contradicts what might be expected from an oxygen-doped sample, as it is well known

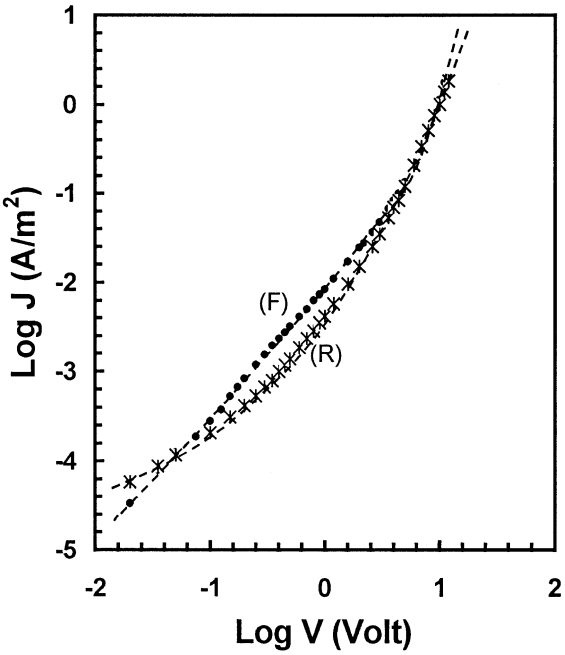

Fig. 4. Typical *J–V* characteristics obtained from an Au/NiPc/In sample after it has been exposed to dry air for a period of 3 days. For forward (F) and reverse (R) bias.

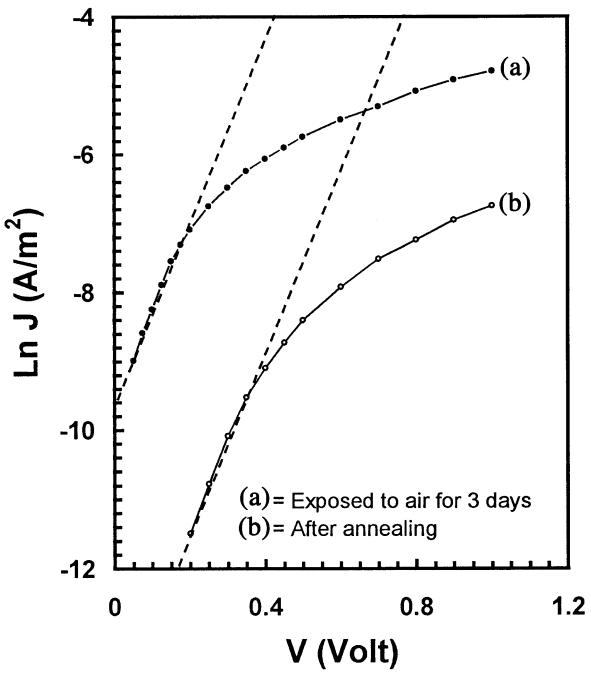

Fig. 5. Semi-logarithmic plot of the forward bias *J–V* characteristic obtained from an Au/NiPc/In sample: (a) after exposure to dry air for 3 days and (b) after annealing at 393 K.

that oxygen acts as an acceptor level for most Pcs [4], therefore an increase in conductivity should be expected. The RR of the cells at ± 1 V, was ≈ 2. This value is 40 times lower than the value obtained for the same sample under vacuum. Therefore, it appears that the formation of the native indium oxide layer and not the presence of O_2 within the NiPc layer is the dominant factor that determines rectification properties of the device. The forward bias characteristic of Fig. 4 has been re-plotted in the form of ln (J) vs. V, and is shown in Fig. 5 (curve A). As can be seen within the voltage region of 0.075–0.2 V, J follows the thermionic emission model described by Eq. (1). Analysis of curve (A) yield the values for $J_S = 6.77 \times 10^{-5}$ A m^{-2} and $\phi_b = 0.82$ eV. The value for n was also deduced from the slope of the linear portion of the ln (J) vs. V curve in Fig. 5 (curve a), yielding a value of 2.74. Although, the magnitude of ϕ_b has remained approximately the same as that obtained from the sample tested under vacuum, the value of n has increased by a factor of 1.44. This departure from ideal behaviour may also be attributed to the presence of an interfacial oxide layer. Such an oxide layer will create a bias dependence of the barrier height and consequently change the shape of the *J–V* characteristic. The latter will be manifested as an increase in the value of n. Additional experimental evidence of the existence of an interfacial oxide layer are provided by the reduction of current flowing through the device. This observation is in agreement with results obtained for inorganic devices where the presence of an interfacial oxygen layer with thickness of only few single layers (≈ 2 nm) caused an increase of the ideality factor n from 1 to 1.3–1.5 [27]. For bias voltage levels of $V > 4$ V, the forward *J–V* curve in Fig. 4, is characterised by a logarithmic slope of ≈ 3, indicating a SCLC mechanism governed by an exponential trap distribution. Therefore, using Eqs. (6) and (8) the following trap parameters were evaluated: $l = 2.2$, $T_t = 650°$ K, $P_0 = 8.7 \times 10^{46}$ J^{-1} m^{-3}, and $N_{t(e)} = 7.8 \times 10^{26}$ m^{-3}. The value for $N_{t(e)}$ obtained in the present case is significantly higher than the value derived for the same sample tested under vacuum. It is believed that this increase is associated with oxidisation of the In electrode, giving rise to a space charge region where trapping of holes near O_2 ions occurs. The reverse bias characteristics of Fig. 4, plotted in the form of ln (J) vs. $V^{1/2}$ are shown in Fig. 6 (curve a). Similar to the reverse bias characteristic of Fig. 3, Fig. 6 (curve a) also exhibits two distinct linear regions. The value of β calculated from the slope of the low voltage region, was found to be 9.28×10^{-5} eV m$^{1/2}$ V$^{-1/2}$. This value is also at variance with that expected for the Schottky effect being four times higher. In the higher voltage range, however, the derived value of β is in very good agreement with that expected for the Poole–Frenkel effect, being 0.9 times the theoretical value of β_{PF}, suggesting a bulk limited conduction process. The presence of an interfacial oxide layer is also believed to be the cause for the low value of RR obtained in the present case. Card and Rhoderick [28] have shown that the reverse current of

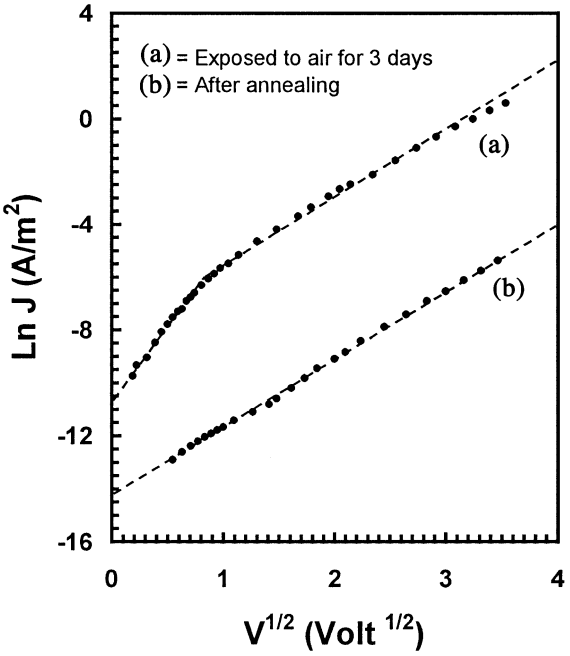

Fig. 6. Semi-logarithmic plot of the reverse *J–V* characteristic obtained from an Au/NiPc/In sample: (a) after exposure to dry air for 3 days and (b) after annealing at 393 K.

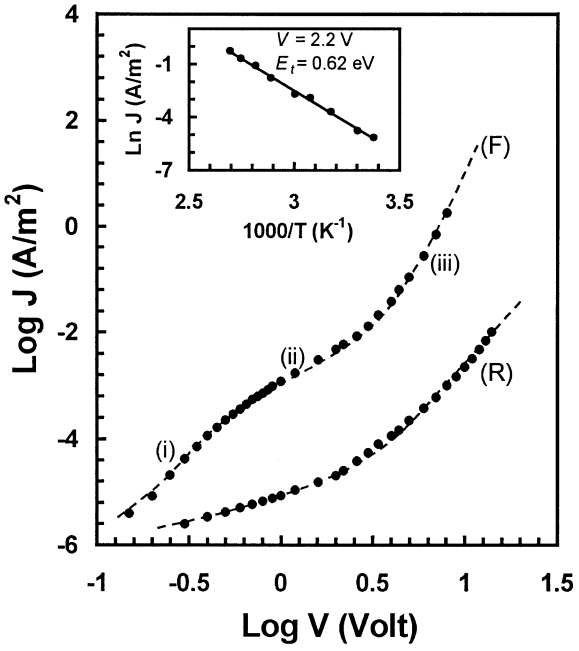

Fig. 7. Typical set of the *J–V* characteristics obtained from the oxygen doped Au/NiPc/In sample after thermal annealing at 393 K for approximately 20 min. For forward (F) and reverse (R) bias.

a diode with a fairly thick interfacial layer may actually be greater than the current flowing through a diode with a very thin oxide layer.

3.3. Heat-treated samples

The effects of annealing on the electrical characteristics of the oxygen doped Au/NiPc/In devices were investigated. The temperature reached during annealing process was 393 K, and was maintained for approximately 20 min. The sample was then left to cool down to room temperature under high vacuum conditions. The *J–V* characteristics obtained from a typical device are shown in Fig. 7. It is seen that conduction exhibits strong polarity dependence with RR = 152 at ± 1 V, while the semi-logarithmic *J–V* plot of the forward bias characteristic, also shown in Fig. 5 (curve b), accords with Eq. (1). Following similar analysis that was described in Section 3.1 values for $J_S = 4.56 \times 10^{-7}$ Am^{-2}, $\phi_b = 0.95$ eV and $n = 2.58$ were obtained. These values are higher than those derived from the same sample tested under vacuum. The high value of n may be attributed to the presence of a thin interfacial oxide layer at the In/NiPc interface, and has been discussed in an earlier subsection. Since ϕ_b depends on the Fermi level of the NiPc, additional increase in its magnitude is attributed to adsorbed molecules of oxygen remaining on the NiPc layer after heat-treatment of the samples. A fuller analysis on the influence of O_2 on rectification properties of NiPc devices has been reported by the authors elsewhere [29]. Similar to the forward bias characteristic in Fig. 1, the forward bias characteristic of Fig. 7 shows two different power law exponents. For applied voltages in the range of 1.2–2.6 V, a quadratic dependence of J with V was observed. Analysis of the curve yields values for $\theta = 7.73 \times 10^{-8}$ and $N_{t(e)} = 2.78 \times 10^{23}$ m^{-3}. Energetic position of the single trapping level within the forbidden band gap ($E_t = 0.62$ eV) was calculated from the current temperature measurements shown in the left-hand corner of Fig. 7. For bias voltages ($V > 5$ V), a super-quadratic dependence of $J \propto V^{5.93}$ was evident. Following the same arguments as in Section 3.1 (for the forward bias characteristic of Fig. 1 region ii), the trap parameters associated with region (ii) of the forward bias characteristics of Fig. 7 were calculated yielding: $l = 4.93$, $T_t = 1445°$ K, $P_0 = 6.17 \times 10^{43}$ J^{-1} m^{-3} and $N_{t(e)} = 1.23 \times 10^{24}$ m^{-3}. Fig. 7 also shows the reverse bias characteristic (curve R) for the annealed Au/NiPc/In sample. The current density in this case is considerably lower than in the forward bias direction. The reverse bias characteristic has been re-plotted in the form of ln (J) vs. $V^{1/2}$ and is also shown in Fig. 6 (curve b). The value of β calculated from the gradient of the curve was $\sim 4.62 \times 10^{-5}$ eV m$^{1/2}$ V$^{-1/2}$. Although, the value of β obtained in the present case is approximately equal to that expected for Poole–Frenkel emission, it is believed that conduction is dominated by an electrode limited conduction mechanism.

4. Summary and conclusions

In this paper we have described the electrical properties of Au/NiPc/In thin film devices prior and after exposure to dry air. The effects of heat treatment on the electrical properties of oxygen doped devices were also investigated. It is found from the dark *J–V* characteristics, for samples maintained under high vacuum, that NiPc form Schottky barriers with indium electrodes. For higher electric fields a transition from electrode limited to bulk limited conduction was observed. Upon exposure of the sample to dry air, RR decreases while the diode ideality factor (n) increases. This behaviour has been attributed to the formation of a thin oxide layer at the NiPc/In interface. Heat treatment of the sample devices leads to the increase of the contact potential and a slight drop in the diode ideality factor. Conduction in the reverse bias for this type of sample is found to be dominated by a current limitation mechanism originated at the NiPc/In interface.

References

[1] G. Guillaud, J. Simon, J.P. Germain, Coordination Chem. Rev. 178-180 (1998) 1433.
[2] K.Y. Law, Chem. Rev. 93 (1993) 449.

[3] A. Fujii, Y. Ohmori, K. Yoshino, IEEE Trans. Electron Devices 44 (8) (1997) 1204.
[4] R.D. Gould, Coordination Chem. Rev. 156 (1996) 237.
[5] F.-R. Fan, L.R. Faulkner, J. Chem. Phys. 69 (7) (1978) 3341.
[6] T.S. Shafai, R.D. Gould, Int. J. Electron. 73 (1992) 307.
[7] R.O. Loutfy, J.H. Sharp, C.K. Hsiao, R. Ho, J. Appl. Phys. 57 (1981) 5218.
[8] T.G. Abdel-Malik, R.M. Abdel-Latif, A.E. El-Samahy, S.M. Khalil, Thin Solid Films 256 (1995) 139.
[9] G.D. Sharma, S.G. Sangodkar, M.S. Roy, Mater. Sci. Eng. B41 (1996) 222.
[10] S. Gravano, A.K. Hassan, R.D. Gould, Int. J. Electron. 70 (1991) 477.
[11] R.D. Gould, J. Phys. D: Appl. Phys. 9 (1986) 1785.
[12] T.D. Anthopoulos, T.S. Shafai, Phys. Stat. Sol. (a) 181 (2) (2000) 569.
[13] M.S. Sze, Physics of Semiconductor Devices, 2nd ed., Wiley, New York, 1981.
[14] A. Rose, Phys. Rev. 97 (1955) 1538.
[15] A. Sussman, J. Appl. Phys. 38 (1967) 2738.
[16] K.F. Schoch, J. Greggi, T.A. Temofonte, J. Vac. Sci. Technol. (A) 6 (1) (1988) 155.
[17] M.A. Lampert, Rep. Prog. Phys. 27 (1964) 329.
[18] R.D. Gould, M.S. Rahman, J. Phys. D 14 (1981) 79.
[19] R.D. Gould, J. Appl. Phys. 53 (1982) 3353.
[20] T.G. Abdel-Malik, Int. J. Electron. 72 (3) (1992) 409.
[21] R.D. Gould, R.I. Blyth, Phys. Stat. Sol. (a) K57 (1990) 120.
[22] J.G. Simmons, J. Phys. D 4 (1971) 613.
[23] A.S. Riad, M. El-Shabasy, R.M. Abdel-Latif, Thin Solid Films 235 (1993) 222.
[24] F.-R. Fan, L.R. Faulkner, J. Chem. Phys. 69 (7) (1978) 3334.
[25] R.D. Gould, A.K. Hassan, Thin Solid Films 193/194 (1990) 895.
[26] R.D. Gould, C.J. Bowler, Thin Solid Films 164 (1988) 281.
[27] E.H. Rhoderick, R.H. Williams, Metal-Semiconductor Contacts, Clarendon Press, Oxford, 1988.
[28] H.C. Card, E.H. Rhoderick, J. Phys. D: Appl. Phys. 4 (1971) 1602.
[29] T.D. Anthopoulos, T.S. Shafai, 8th International symposium on Electron Devices for Microwave and Optoelectronic applications (EDMO), IEEE, University of Glasgow, (2000) 179.